

**GA-A22679**

**PROSPECTS FOR CORE HELIUM DENSITY  
AND RELATED MEASUREMENTS ON ITER  
USING ACTIVE CHARGE EXCHANGE**

**by**

**D.M. THOMAS, K.H. BURRELL, M.R. WADE, and R.T. SNIDER**

**SEPTEMBER 1997**

## DISCLAIMER

This report was prepared as an account of work sponsored by an agency of the United States Government. Neither the United States Government nor any agency thereof, nor any of their employees, makes any warranty, express or implied, or assumes any legal liability or responsibility for the accuracy, completeness, or usefulness of any information, apparatus, product, or process disclosed, or represents that its use would not infringe privately owned rights. Reference herein to any specific commercial product, process, or service by trade name, trademark, manufacturer, or otherwise, does not necessarily constitute or imply its endorsement, recommendation, or favoring by the United States Government or any agency thereof. The views and opinions of authors expressed herein do not necessarily state or reflect those of the United States Government or any agency thereof.

**PROSPECTS FOR CORE HELIUM DENSITY  
AND RELATED MEASUREMENTS ON ITER  
USING ACTIVE CHARGE EXCHANGE**

by

**D.M. THOMAS, K.H. BURRELL, M.R. WADE,\* and R.T. SNIDER**

This is a preprint of a paper presented at the Workshop for Diagnostics for ITER on September 4–12, 1997 in Varenna, Italy, and to be published in the *Proceedings*.

\*Oak Ridge National Laboratory, Oak Ridge, Tennessee.

**Work supported by  
the U.S. Department of Energy under  
Contract Nos. DE-AC03-94SF20282 and DE-AC05-96OR22464**

**GA PROJECT 3994  
SEPTEMBER 1997**

## **PROSPECTS FOR CORE HELIUM DENSITY AND RELATED MEASUREMENTS ON ITER USING ACTIVE CHARGE EXCHANGE**

D.M. Thomas, K.H. Burrell, M.R. Wade,\* R.T. Snider

General Atomics  
P.O. BOX 85608  
San Diego, CA 92186-5608

\*Oak Ridge National Laboratory  
P.O. Box 2009  
Oak Ridge, TN 37831

### **ABSTRACT**

The measurement of low-Z impurities, in particular He ash, in the core of International Thermonuclear Experimental Reactor (ITER) remains an outstanding diagnostic issue. The only credible candidate at present is active charge exchange recombination spectroscopy (CER) utilizing a diagnostic neutral beam (DNB) optimized for the dual requirements of beam penetration and charge exchange cross section, resulting in beam energies of  $\sim 100$  keV/AMU. Using the existing ITER parameter profile and equilibrium data files and reasonable assumptions regarding viewing optics and DNB performance, we have employed a benchmarked multistep beam penetration code to yield signal-to-noise estimates for possible core helium concentration measurements. These studies confirm the importance of precise determination of beam intensities via accurate modeling and independent measurement, as well as the need for beam modulation, to satisfy the stated measurement precisions needed for ITER. Comparable calculations have been done for an intense pulsed neutral beam based on ion diode technology, as well as other candidate He-CER wavelengths, to assess the relative advantages of these techniques. Since any DNB-based diagnostic system actually deployed on ITER will likely be used for a variety of purposes, signal-to-noise calculations for the related active CER measurement of ion temperatures have also been performed and will be presented.

### **1. INTRODUCTION**

Active plasma spectroscopy, or spectroscopy based upon local signal enhancement via a penetrating neutral atomic beam, is employed as a key diagnostic on almost all present-day tokamaks. This technique is utilized for a wide variety of measurements in the plasma edge and core, including ion temperature [via Doppler broadening of intrinsic impurity lines which are efficiently populated by charge exchange from beam atoms — charge exchange recombination spectroscopy (CER)], plasma rotation (via Doppler shift of the same impurity lines), and impurity profile information (via quantitative spectroscopy of the impurity line intensities). Other important measurements that can be undertaken with active spec-

troscopy include plasma turbulence levels [via fluctuation analysis of the collisionally excited beam emission — beam emission spectroscopy (BES)] and local magnetic/electric field determination [via polarimetry of the beam emission polarization state induced either by the motional Stark or Zeeman effect (MSE)].

These measurements, all variations of a theme, have substantially increased our knowledge of the behavior and optimization of fusion plasma experiments. Our present picture of core and edge barrier transport formation based on shear suppression of turbulence owes its basic experimental underpinnings to well designed and deployed active spectroscopy systems.<sup>1–3</sup> Similarly, studies of core helium ash formation and transport, and the performance of pumped divertors for helium exhaust, have benefited from the precise, local, absolute measurements possible using this technique.<sup>4,5</sup>

Adoption of active spectroscopy for the International Thermonuclear Experimental Reactor (ITER) represents a challenging opportunity. As discussed in previous contributions to this workshop<sup>6,7</sup> there are numerous obstacles to deployment, the two most important of which are as follows:

1. The large size of ITER compared to present experiments implies much longer beam propagation path lengths resulting in severe attenuation of the neutral beam as it penetrates to the core region. One cannot simply go to higher energies to improve this situation. As pointed out,<sup>6,7</sup> the energy dependence of the beam attenuation and charge exchange cross sections results in an optimal beam energy of  $\sim 100\text{--}150$  keV/AMU. The substantially longer path lengths through the plasma for the viewing chords imply any spectroscopic measurement, whether active or passive, will have to be made in the presence of a substantial bremsstrahlung background, typically several orders of magnitude larger than the desired charge exchange or emission line intensity. This implies that any usable system must have extremely good dynamic range and low noise.
2. The ignited phase of ITER will create an intense radiation zone around the device. Measurements in this environment will require diagnostic immunity/resistance to neutron and gamma radiation at a level substantially beyond present day experiments. Relevant issues include the radiation hardening of optical elements and detectors, including the survivability/distortion/erosion of first wall optical elements which will be required for any reasonable measurement. In addition, this same environment demands the utmost in reliability and remote maintenance capability from the diagnostic; aspects which are relatively less important (and hence less developed) on existing experiments.

Despite these obstacles, substantial design and development work continues on active spectroscopy systems for ITER because of the unique information they can provide on core plasma conditions. In the case of core helium density measurements — a crucial indicator of the success of ITER — no credible alternative to CER has emerged. In this paper we expand on previous work<sup>6,7</sup> to present a detailed performance estimate for a diagnostic system appropriate for measurements of core helium concentrations in the ITER environment, based upon active spectroscopy of the  $4\text{--}3$  He II transition. In Section 2 we review the desired measurement resolutions and relevant ITER geometry to arrive at a realistic layout for the diagnostic. Section 3 describes several ITER profile scenarios based upon the existing ITER parameter profile and equilibria data files and lists the assumed values for the diagnostic neutral beam (DNB) performance. Section 4 covers the calculations of expected beam intensities and signal-to-noise ratios, based on a benchmarked multistep beam attenuation code<sup>8,9</sup> and the various profile scenarios. Section 5 discusses the advantages associated with using a pulsed beam based on ion diode technology as opposed to the baseline DNB design. In Section 6 we investigate the possible benefit of using an alternative wavelength — the  $5\text{--}4$  He II transition in the infrared — for the helium concentration measurements. We discuss the prospects for ion temperature and rotation measurements using active CER in Section 7. In Section 8 a summary and some conclusions are presented.

## 2. ITER PARAMETERS AND REQUIREMENTS

The following diagnostic requirements are based upon the minutes of the ITER Diagnostic Expert Group Meeting (3/96):

These four parameters represent zeroth, first, and second order moments of the intensity distribution of the emitted He line. We note the fourth parameter listed — ion temperature — will be the most difficult measurement in terms of satisfying the quoted requirements, since the spectrum must be resolved sufficiently. The requirement for measuring plasma rotation demands orthogonal views of the beam, implying a vertical viewport must be considered a necessary part of this diagnostic system. The helium density profile measurement requires an absolute intensity calibration. This calibration must be maintained across the substantial number of viewing chords needed to satisfy the spatial resolution requirements. In Table 2 we lists what are believed to be reasonable parameters for a prototypical active CER system, based on the most recent engineering layouts and dimensions. The number of chords permits good coverage of the minor radius region 0.2–2.7 m (Fig. 1). The auxiliary chords for monitoring beam emission  $H_{\alpha}$  serve as a crucial experimental cross-check of the beam attenuation calculations, which are sensitively dependent on local impurity densities and accurate cross sections. It may be desirable to have additional  $H_{\alpha}$  channels having higher spatial resolution to accurately determine the lateral dimensions of the beam *in situ*. The auxiliary visible bremsstrahlung measurements at the He wavelength displaced laterally from the beam serve as a cross-check on the beam calculations.

**Table 1.** ITER requirements for active CER measurements.

Parameter	Range	Required (Spatial) (cm)	Resolution (Temporal) (ms)	Required Accuracy (%)
Core helium density (Category 2)	1%–20%	30	100	10
Toroidal plasma rotation (Category 1)	1–200 km/s	~5	10	30
Poloidal plasma rotation (Category 1)	1–50 km/s	~5	10	30
Ion temperature profile (Category 2)	0.5–50 keV	30	100	10

**Table 2.** Strawman active spectroscopy system parameters.

Number of optical penetrations	10 (5 vertical, 5 tangential)
Size of individual penetration	0.2 m × 0.2 m
Total estimated penetration area	0.4 m <sup>2</sup>
Number of sightlines, total	128
Number of tangential sightlines	40 CER signal 14 $H_{\alpha}$ 10 Background
Number of vertical sightlines	40 CER signal 14 $H_{\alpha}$ 10 Background
Collection area of first mirror	0.2 m × 0.2 m
Characteristic chord length	~16 m
Presumed emission area-toroidal view	0.2 m vertical × 0.05 m radial
presumed emission area-vertical view	0.2 m toroidal × 0.05 m radial
Collection solid angle, first mirror	$4.9 \times 10^{-4}$ sr
Etendue through spectrometer (est.)	$2 \times 10^{-7}$ m <sup>2</sup> -sr

### 3. PROFILES AND OPERATIONAL SCENARIOS

For the calculations presented here, we have used flat and peaked reference profiles from the ITER database<sup>10</sup> (Fig. 2). The relevant  $T_e$ ,  $n_e$ ,  $Z_{\text{eff}}$ , etc. profiles were first mapped to minor radius using the associated equilibria to provide suitable inputs for the beam attenuation and rate equation codes. We have assumed two cases for the study. The first is a steady state case represented by the flat profile, and assuming a constant (with density) 10% helium fraction. The second is an early ignition case, where we assume a 1% helium fraction at the core that falls off radially like the temperature profile.

#### DNB Projected Performance

A separate diagnostic neutral beam (DNB) design is crucial to the success of the above measurement. For our calculations we have relied on the provisional design parameters from Ref. 11, summarized in Table 3. Options to increase the design beam energy to 125–150 keV are being pursued. We also note the measurement time limitation, which serves to minimize the overall neutralizer gas flow into the plasma, will serve as a fundamental limit on any active spectroscopy measurements. Finally, the quoted footprint size may be somewhat optimistic based on present technology.

### 4. MULTISTEP BEAM PENETRATION MODELING

Modeling and estimation of the observed helium signal depends crucially on accurate cross sections and rates for beam attenuation and helium emission. We have adapted a previously benchmarked multistep collisional-radiative model<sup>8,9</sup> for the specific ITER geometry, profile conditions, and putative DNB parameters. The code uses the most recent collisional rates available from the Atomic Data and Analysis Structure (ADAS) database.<sup>12</sup> Initial runs verified the importance of the multistep corrections to beam attenuation calculations, with attenuation enhancement factors from 6–8 found compared to the earlier single-step estimates.<sup>6</sup> For the energy range of interest, attenuation factors of  $10^{-3}$  to  $10^{-4}$  are common for the core region  $\rho_{\text{min}} \leq 0.5$  m ( $\rho \leq 0.1$ ).

The helium emissivity based on the calculated source strength, along with the competing bremsstrahlung, is then calculated using the assumed geometrical factors from Tables 2 and 3. Figure 4 shows the results for the startup and fully ignited cases.

The signal-to-noise of the He II CER measurements may be estimated under the following assumption: for the no competing lines case we presume the fluctuations in the continuum background to be the dominant noise source. Then the SNR will be given by<sup>6,7</sup>

$$\text{SNR} = \frac{N_{\text{He}}}{\sqrt{N_{\text{B}} + N_{\text{He}}}} = \frac{S_{\text{He}} \Delta t \text{DF}}{\sqrt{R S_{\text{He}} \Delta t \text{DF}}} = \frac{S_{\text{He}} \Delta t \text{DF}}{\sqrt{(S_{\text{He}} \Delta t)(R + \text{DF})}} = \frac{\sqrt{S_{\text{He}} \Delta t \text{DF}}}{\sqrt{(R + \text{DF})}} \quad (1)$$

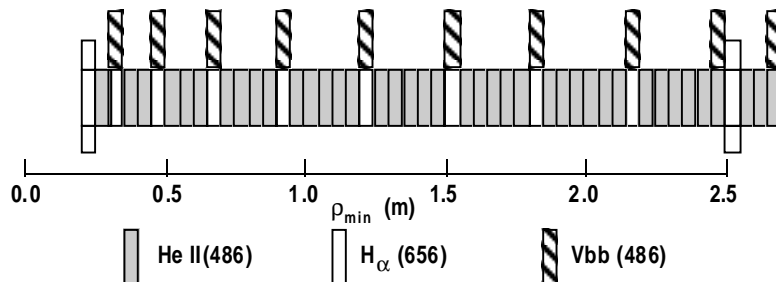


**Figure 1.** Possible layout of viewing geometry, showing the 64 He CER, Ha BES, and VBB (visible bremsstrahlung) locations. The basic element dimensions are 20 cm (lateral) by 5 cm (vertical), and are presumed superimposed on the beam trajectory. Two orthogonal arrays — one vertical, one toroidal — are presumed, for a total of 128 discrete spatial points.

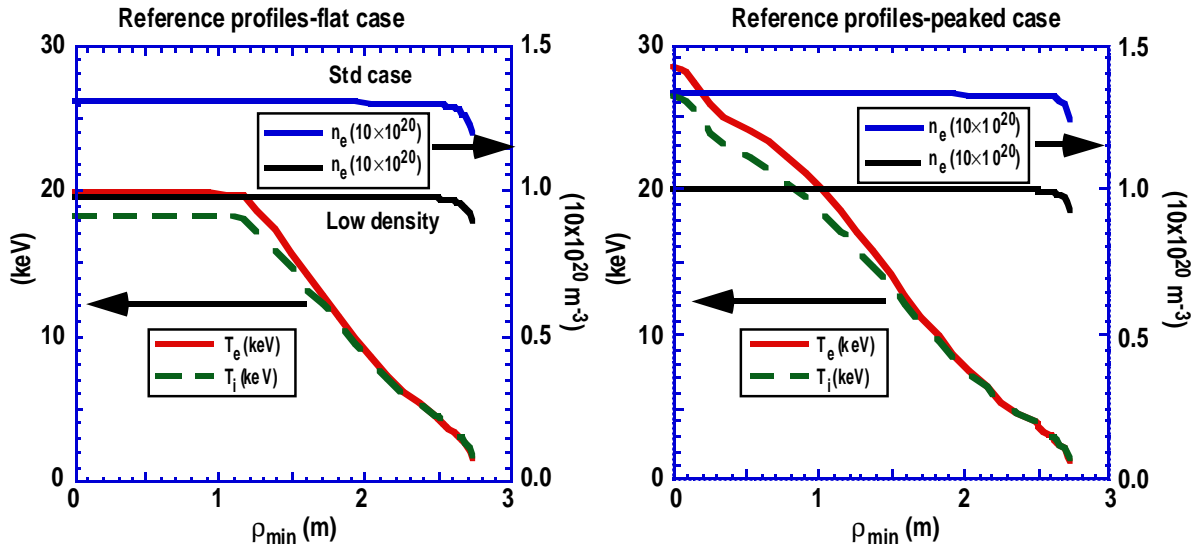


**Figure 2.** Reference profiles extracted from the ITER profile database, showing density, ion and electron temperatures for flat and peaked temperature profile scenarios. The “low density” ( $\sim 1.0 \times 10^{20} \text{ m}^{-3}$ ) cases are most relevant to planned ITER operation.  $Z_{\text{eff}}$  profiles for all cases were reasonably flat with  $Z_{\text{eff}} \sim 1.5$ .

**Table 3.** Provisional parameters of diagnostic neutral beam<sup>11</sup>

Beam species	$\text{H}^0$
Beam energy (keV)	100
Neutral equivalent current (A)	50
Beam power (MW)	5
Beam divergence	$0.2^\circ$
Beam footprint at beam focus	$0.2 \times 0.2 \text{ m}^2$
Beam focus	At $r/a = 0.3\text{--}0.4$
Equivalent $\text{H}^0$ density at focus (unattenuated)	$1.78 \times 10^{15} \text{ m}^{-3}$ ( $\sim 2 \times 10^{-4} n_e$ )
Beam modulation frequency (Hz)	5 (0.1 s on, 0.1 s off)
Measurement time (s)	1–3 every 10–20

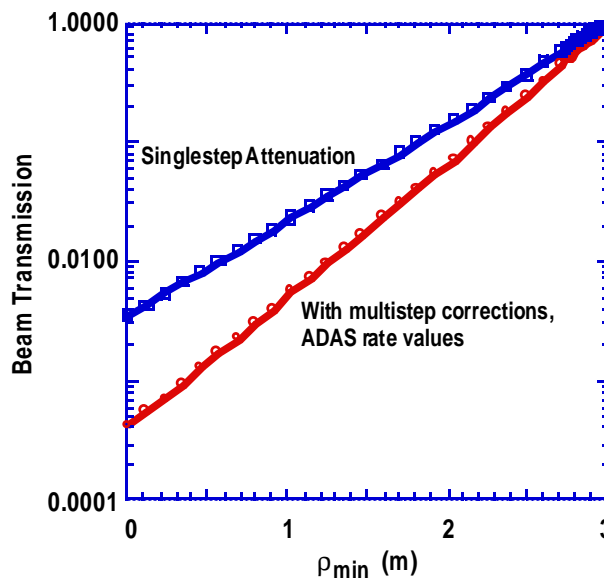


**Figure 3.** Calculation of 125 keV  $\text{H}^0$  neutral beam transmission for the ITER flat profile case (scenario 1), using a simple single step and full multistep attenuation calculations.



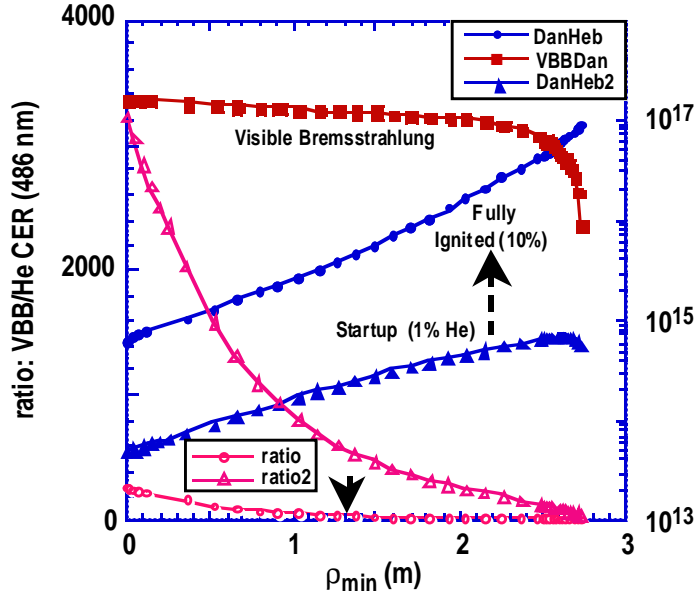


**Figure 4.** He CER and bremsstrahlung emissivities at 468 nm for the startup and fully ignited scenarios. Also plotted are the emissivity ratios for the two times. Beam energy = 125 keV, assumed neutral current density of  $10^3$  A/m<sup>2</sup> (40 A neutral equivalent current).

where  $S_{\text{He}}$  = helium intensity,  $R = \text{VBB/He}$  intensity ratio,  $\Delta t$  = integration time and  $DF =$  duty factor for beam. Calculations were performed for the two cases assuming a 50% duty cycle and 100 ms integration time — the cited time requirement. We note the 5 Hz DNB modulation frequency in Table 3 will permit four 50 ms timeslices (two signal and two background) per beam cycle. Longer integration times improve the SNR as  $\sqrt{\Delta t}$ . Figure 5 shows the results for the startup and fully ignited cases. For the calculation of absolute signal levels we have assumed the etendue and other optical parameters listed in Table 2.

The values of SNR found are marginal (for the desired time resolution) at the smaller radii, especially if we are interested in tracking the buildup of helium at the beginning of the ignited phase. The situation will be even more marginal for ion temperature and rotation measurements, or for plasma densities higher than those presumed in the modeling.

## 5. PULSED BEAM PROSPECTS

Because of the narrow limits set on the beam energy by the penetration and charge exchange requirements, the principal beam improvement that could be made would be an increase in current density. A substantial improvement in SNR would result from the deployment of an intense pulsed neutral beam based upon ion diode technology.<sup>13</sup> Figure 6 shows the calculated improvement from a hypothetical 100 keV, 50 kA IDNB, presuming the same beam footprint as for the conventional beam. Such beams are close (within a factor of about two) to satisfying the intensity and divergence requirements; remaining issues include beam repetition rate and effective neutralization. The use of these beams would improve the SNR at the stated time resolutions by factors of 10–20 in the core.

Especially for the temperature measurements, the increase in SNR will probably be necessary. A side benefit of the pulsed beam concerns the relative ease of fitting the line-shape: the technique of using background subtraction to reject edge He II emission will be far more effective on the 1  $\mu$ s timescale, and the peaks may be better fit by a single Gaussian representing the hot core CER signal.

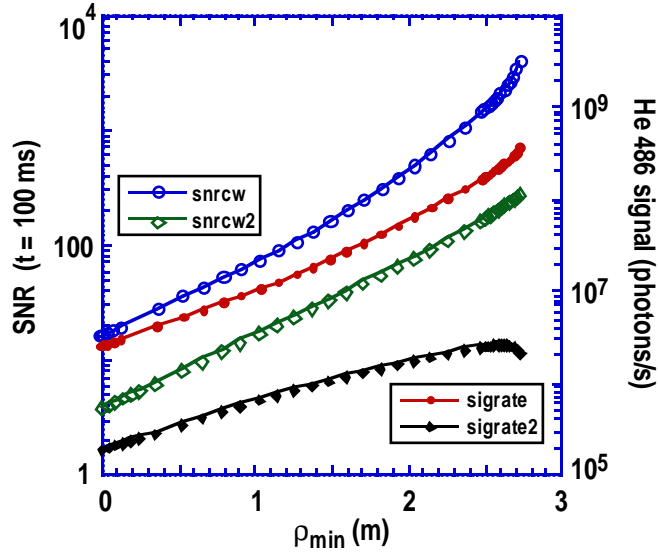


**Figure 5.** SNR estimates (and the associated signal levels in photons/s) based on the preceding beam calculations. Integration time 100 ms, 50% duty cycle. An overall system etendue of  $2 \times 10^{-7}$ , optical efficiency of  $1 \times 10^{-2}$ , and bandwidth of 2 nm is assumed in the calculations. Beam energy = 125 keV, assumed neutral current density of  $10^3$  A/m<sup>2</sup> (40A neutral equivalent current). Snrcw = SNR for startup, snrcw2 = SNR for fully ignited case. Sigrate2 = signal level for startup, sigrate = signal level for fully ignited case.

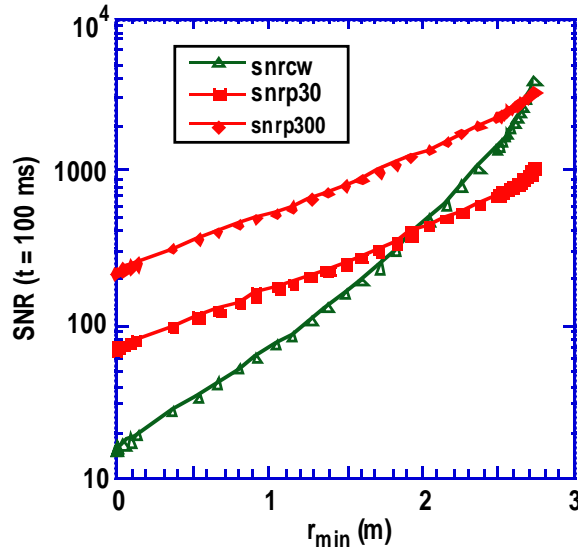


**Figure 6.** SNR estimates for a 1  $\mu$ s 50 kA pulsed ion diode neutral beam (IDNB), compared to the conventional DNB for the fully ignited scenario. The two cases shown are for 30 pps and 300 pps rep rates. Integration time 100 ms, 50% duty cycle. An overall system etendue of  $2 \times 10^{-7}$ , optical efficiency of  $1 \times 10^{-2}$ , and bandwidth of 2 nm is assumed in the calculations. Conventional beam parameters: energy = 125 keV, assumed neutral current density of  $10^3$  A/m<sup>2</sup> (40A neutral equivalent current).

## 6. THE He-II 5-4 TRANSITION

One possible improvement for the helium intensity measurement involves the use of alternative wavelengths to the standard 486 nm  $N = 4 \rightarrow 3$  transition of He II. In particular, the  $N = 5 \rightarrow 4$  transition of He II offers several potential advantages. This near-infrared ( $\lambda = 1012.3$  nm) line is also efficiently created by the charge exchange process and can be efficiently detected using present day technology. Figure 7 shows the two rate coefficients for Scenario 1 as a function of beam energy. For the energies of interest, the ratio of  $\langle \sigma v \rangle_{4-3}$  to  $\langle \sigma v \rangle_{5-4}$  is about 2.4 for the entire plasma profile.

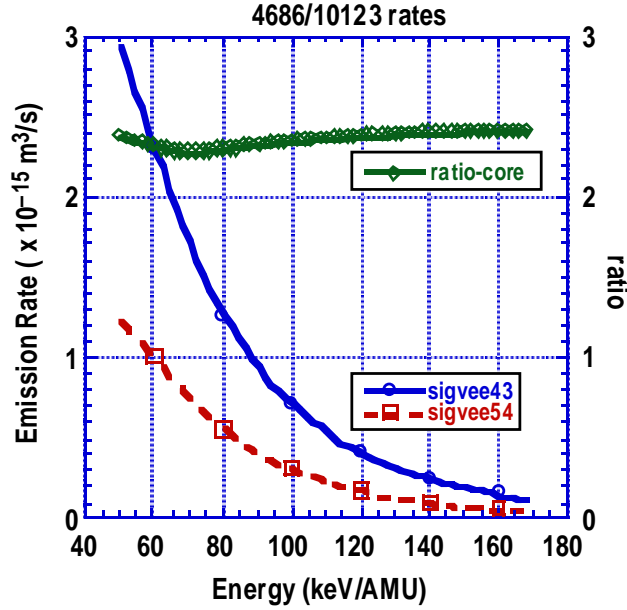


**Figure 7.** Emission rates for the 468.6 nm and 1012.3 nm transitions in He II as an injection energy function for the ITER flat profile case (Scenario 1). The ratio  $\langle\sigma v\rangle_{4-3}/\langle\sigma v\rangle_{5-4}$  is also plotted.

Because of the  $\lambda^{-2}$  dependence of the bremsstrahlung intensity, the competing background light would be expected to drop by a factor of  $(\lambda_{\text{NIR}}/\lambda_{\text{VIS}})^{-2} \sim 4.6$ . Since the required Doppler measurements will also scale with wavelength, an improvement of  $\lambda_{\text{NIR}}/\lambda_{\text{VIS}} \sim 2.2$  in the SNR should be obtained. This effect directly compensates for the somewhat lower emission rate for the  $5 \rightarrow 4$  transition.

Detection of the 1012.3 nm radiation can be accomplished using e.g., silicon APDs; at room temperature the quantum efficiency is  $\sim 70\%$ .<sup>14</sup> These devices are presently used with great success for Nd:YAG Thomson scattering measurements on DIII-D at greater wavelengths ( $\lambda < 1100$  nm).<sup>15</sup> Temperature stabilization of both detector and electronics is crucial for this application. We have observed both lines simultaneously on DIII-D discharges using cooled silicon CCD detectors.<sup>16</sup> In this case the system was not specifically designed for high NIR sensitivity and the quantum efficiency is about 10% at the  $5 \rightarrow 4$  transition frequency. Germanium or other infrared detectors may be considered.

The use of the longer wavelength has two additional advantages related to the optical system. First, the transmission efficiency through previously irradiated optical fibers is seriously diminished<sup>17</sup> in the visible. As it turns out the transmission is substantially better in the NIR<sup>18</sup> which would lead to relatively larger and less distorted measurements. Second, the longer wavelength will be more efficiently reflected from the metal mirrors used for the collection optics, and should be less affected by the surface coating, radiation damage and erosion which will inevitably occur to the plasma-facing mirrors.

For either transition wavelength, there are competing transitions due to the other light impurity ions, specifically C and Be (Table 4). Although we hope the absolute concentrations of these species will be low there may be enough to complicate the analysis of the He line. We are presently examining the relative scalings of these higher-n transitions to see if this represents an additional advantage for the  $5 \rightarrow 4$  transition.

Table 4. Relevant impurity transitions for helium measurements.

Ion Species	468.6 nm	1012.3 nm
He II	4 $\rightarrow$ 3	5 $\rightarrow$ 4
Be IV	8 $\rightarrow$ 6	10 $\rightarrow$ 8
C VI	12 $\rightarrow$ 9	15 $\rightarrow$ 12

## 7. ION TEMPERATURE/ROTATION MEASUREMENTS

As mentioned earlier, in contrast to the basic intensity measurement necessary for calculating the helium concentration, determining the ion temperature and rotation requires spectral analysis and fitting of the Doppler-broadened emission line — in effect taking higher order moments of the spectral distribution. The degradation in SNR was earlier estimated<sup>6</sup> by presuming an increase in 10 in the required spectral resolution (to 0.2 nm) leading to a similar loss in the time resolution to recover the SNR. To follow the evolution of temperature and rotation during the plasma startup, or during a core barrier formation period where the temperature may be somewhat lower than the ignited case, it is clear we will require spectral resolutions substantially better than the factor of ten for adequate confidence in the line broadening and line shift values. For example, assuming a 20 km/s resolution requirement for the poloidal field measurement from Table 1 implies a needed spectral resolution  $\Delta\lambda = \lambda(\Delta v/c) = 0.03$  nm in the case of the 486 nm line, a factor of seventy smaller than that for the helium concentration determination. Similarly, a 1 keV resolution at 10 keV ion temperature will require differentiating between spectral halfwidths of roughly 0.90 and 0.86 nm, or 0.04 nm. Since the SNR scales with the square root of the signal intensity, it is clear that the requested time resolutions for temperature and rotation are incompatible with the capabilities of the conventional DNB. The only possible hope with the IDNB is to gate the detection in phase with the pulsed beam. As a reference point, in Fig. 8 we show the SNR estimated for the startup scenario with a 0.04 nm spectral window, assuming the imaging area has been increased by a factor of six to give 30 cm resolution, and 100 ms time resolution as before.

## 8. SUMMARY AND CONCLUSION

Using fairly detailed assumptions about ITER plasma conditions, geometry, and diagnostic neutral beam performance, we have tried to assess the prospects for measuring the core helium concentration profile, and to a lesser extent the ion temperature and plasma

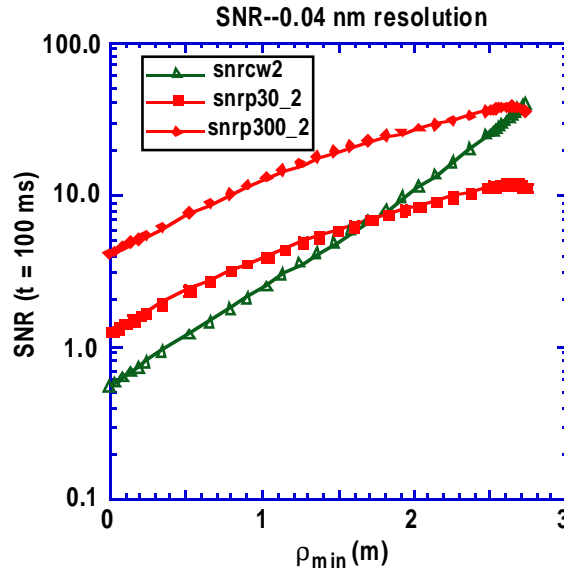


**Figure 8.** SNR estimates for a  $1 \mu\text{s}$  50 kA pulsed ion diode neutral beam (IDNB), compared to the conventional DNB for the startup scenario, using wavelength resolution suitable for temperature or rotation measurement. The radial resolution assumed is 30 cm. The two IDNB cases shown are for 30 pps and 300 pps rep rates. Measurement time 100 ms, 50% duty cycle. An overall system etendue of  $2 \times 10^{-7}$ , optical efficiency of  $1 \times 10^{-2}$ , and bandwidth of 0.04 nm is assumed in the calculations. Conventional beam parameters: energy = 125 keV, assumed neutral current density of  $10^3$  A/m<sup>2</sup> (40 A neutral equivalent current).

rotation profiles, using the visible He II 486.nm line. Using more accurate modelling of beam penetration and charge exchange we have performed signal to noise estimates for the desired measurement precision for the fully ignited case as well as a simple startup case. It is clear that measurements within  $r = 1$  m will be difficult but doable for reasonable optical penetrations and collection efficiencies. However it is also clear that the stated measurement precisions for these parameters, as exemplified in Table 1, are not compatible with the expected DNB performance as listed in Table 3. This argues either for a relaxation of the desired resolution(s), or further work on a pulsed, high current alternative to the conventional DNB, if the more difficult (higher order moment) measurements are to be pursued. The short pulse length of the IDNB also lends itself to short detection gating strategies that should simplify the spectral analysis as well as increasing the SNR. We see that, even for the highest rep rate IDNB case, the  $T_i$  and  $V_{rot}$  measurements will be marginal for the very smallest radii at the highest expected densities. The use of other impurity species, e.g., C or Be is probably not of utility until their concentrations approach a few percent, which is unlikely for the presumed operation of ITER. Finally, the use of an alternate NIR He transition offers some advantages for making these measurements in the ITER environment, and we are continuing to investigate the relative merits of this option.

## 9. ACKNOWLEDGMENTS

Work supported by the U.S. Department of Energy under Contract Nos. DE-AC05-96OR22464 and DE-AC03-94SF20282, Subcontract ITER-GA-4002. The authors have benefited from numerous stimulating and informative discussions with C. Walker, G. Vayakis, V. Mukhovatov, K. Young, E. Marmar, R.C. Isler, and D.G. Whyte.

## References

1. E.J. Strait, et al., Phys. Rev. Lett. **75**, 4421 (1995).
2. F.M. Levinton, et al., Phys. Rev. Lett. **75**, 4417 (1995).
3. K.H. Burrell, Phys. Plasmas **4**, 1499 (1997).
4. D.L. Hillis, et al., Phys. Rev. Lett. **65**, 2382 (1990).
5. M.R. Wade, et al., Phys. Plasmas **2**, 2357 (1995).
6. E.S. Marmar, *Diagnostics for experimental thermonuclear fusion reactors*, P.E. Stott, G. Gorini, and E. Sindoni, ed., Plenum Publishing Corp., New York, 281 (1996).
7. M.G. Von Hellerman, et al., *Diagnostics for experimental thermonuclear fusion reactors*, P.E. Stott, G. Gorini, and E. Sindoni, ed., Plenum Publishing Corp., New York, 321 (1996).
8. W. Mandl, Ph.D. Thesis, University of Munich, JET-IR (92) 05 (1992).
9. D.F. Finkenthal, Ph.D. Thesis, University of California, Berkeley (1994).
10. Profiles courtesy of D. Bouchet and G. Vayakis, ITER-JCT.
11. R. Hemsworth, A. Krylov, M. Hanada, *Proposal of a design of diagnostic neutral beam injector*, ITER Memorandum, December 1996.
12. ADAS documentation set, <http://patiala.phys.strath.ac.uk/adas>.
13. H.A. Davis, et al., Rev. Sci. Instrum. **68**, 332 (1997).
14. P.P. Webb, R.J. McIntyre, Properties of Avalanche Photodiodes, RCA Review, June 1974.
15. C.L. Hsieh, et al., Rev. Sci. Instrum. **61**, 2855 (1990).
16. D.M. Thomas, et al., Rev. Sci. Instrum. **68**, 1233 (1997).
17. D.V. Orlinski, *Diagnostics for Experimental thermonuclear fusion reactors*, P.E. Stott, G. Gorini, and E. Sindoni, ed., Plenum Publishing Corp., New York, 51 (1996).
18. K. Young and A. Ramsey, *Application of fiber optics to present large tokamaks*, Proc. of ITER Technical Meeting of Irradiation Tests on Diagnostic Components, Garching, Germany (1996).